# Liquid water transport and droplet formation and detachment through the gas diffusion layer for PEM fuel cells

**Tamara Whitaker**

**April 19, 2007**

**Professor Jay Benziger**

**Submitted in partial fulfillment of the requirements for the degree of**
**Bachelor of Science in Engineering**

**Department of Chemical Engineering**
**Princeton University**

**This paper represents my own work in accordance with University regulations. I authorize Princeton University to lend this thesis to other institutions or individuals for the purpose of scholarly research.**

**Tamara D. Whitaker**

**I further authorize Princeton University to reproduce this thesis by photocopying or by other means, in total or in part, at the request of other institutions or individuals for the purpose of scholarly research.**

**Tamara D. Whitaker**

**This thesis is dedicated to the women who encouraged me to pursue study in engineering, Jocelyn Harrison, Ph.D. and Zoubeida Ounaies, Ph.D. I appreciate the lessons in research that you taught me so early in my academic career, and I value all of your advice.**

**I would like to acknowledge my advisor and teacher, Professor Jay Benziger for his patience and guidance with this project and throughout my academic career. I owe significant gratitude to the two graduate students who assisted me in setting up my experiments, Erin Kimball and Barclay Satterfield. I would like to acknowledge the Lidow Senior Thesis Fund for supporting my work. Lastly, I would like to acknowledge the professors who have allowed me to work in their research groups over the summers, Professor Ilhan Aksay and Professor Wole Soboyejo.**

# Abstract

In order to ensure that liquid water does not condense in the gas diffusion layer (GDL) and impede the diffusion of the oxygen needed for the electricity-producing reactions, it is required that the gas diffusion layer by hydrophobic. Therefore, it is necessary to apply a hydrostatic pressure in order to force the water to penetrate the pores of the gas diffusion layer. This penetration only happens at the largest pores where the surface energy is smallest, requiring less work to push the water through. Water flow through carbon paper and carbon cloth was observed with a video camera. Once the water penetrates the pore, it forms droplets at the surface of the GDL. As water continues to flow, the droplet increases in size until it reaches a critical size and detaches from the surface of the GDL. In this thesis, a model is presented to understand the physics of this occurrence.

## Table of Contents

## List of Tables

## List of Figures

**Appendix I.** Still images from video recording of water droplets formed on carbon paper.
**Appendix II.** Still images from video recording of water droplets formed on carbon cloth.
**Appendix III.** Design for Flow Visualization cell.

# I. Introduction

There is an increasing interest in the use of polymer electrolyte membrane fuel cells as a power source for both mobile and stationary applications. The first demonstration of a fuel cell was in 1939 by lawyer and scientist William Grove. Since then, much research has been devoted to improving efficiency and lower costs. The proton electrolyte membrane (PEM) fuel cell is being seriously considered as an alternative power source due to its high-energy efficiency, environmentally-friendliness, and simple design [1]. First, fuel cells are generally more efficient than combustion engines; second, there are relatively few moving parts in fuel cells, and the construction is relatively simple. Last, the main by-product of a fuel cell fueled by hydrogen is water. At a time when industrial emissions and emissions from vehicles are being regulated to protect the environment, fuel cells are a very attractive alternative that has been the object of much research. There are still important problems that must be reconciled before fuel cells are a practical solution to energy demands, and more research is needed in order to optimize performance in all conditions and lower costs. The problem of water management in the PEM has attracted much attention.

Fuel cells are multiphase chemical reactors in which two simultaneous chemical reactions are coupled by transport of the intermediate products between catalyst electrodes. The polymer electrolyte membrane (PEM) fuel cell consists of a polymer membrane, in which protons are mobile, sandwiched by the anode and the cathode. A simplified figure of the PEM fuel cell is shown in (Figure 1).

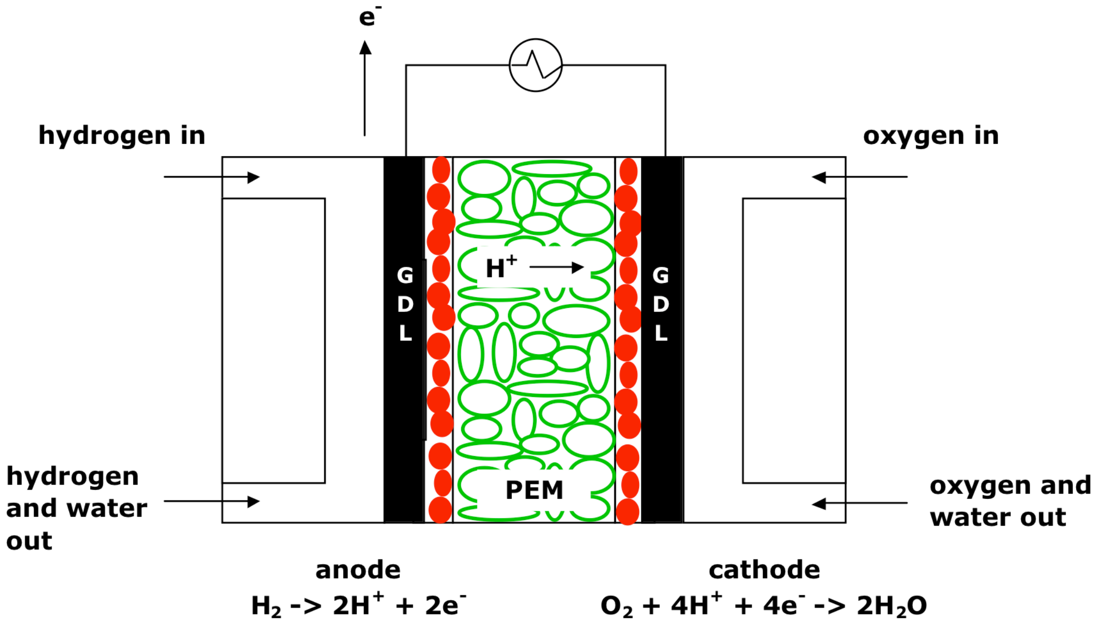

**Figure 1. Hydrogen-oxygen PEM fuel cell. Hydrogen molecules dissociatively adsorb at the anode and are oxidized to protons. Electrons travel through an external load resistance. Protons diffuse through the polymer-electrolyte membrane under an electrochemical gradient to the cathode. Oxygen molecules adsorb at the cathode, are reduced, and react with the protons to produce water.**

Hydrogen gas is fed into the anode gas channel and diffuses through the anode gas diffusion layer, where it comes into contact with the anode catalyst. A platinum catalyst is necessary in order to speed up reaction rates [2]. Each $H_2$ molecule is dissociatively adsorbed and oxidized into two protons that diffuse through the polymer electrolyte membrane to the cathode through an electrochemical gradient according to Equation (1) [3].

$$2H_2 \rightarrow 4H^+ + 4e^- \qquad (1)$$

The resulting electrons are conducted through an external circuit, producing the work. On the cathode side of the cell, oxygen is fed into the gas flow channel, where it diffuses through the cathode gas diffusion layer to the cathode catalyst. Once in contact with the catalyst, each $O_2$ molecule is split into two $O^-$ ions whose negative charge drives positive $H^+$ ions through the membrane according to Equation (2).

$$O_2 + 4e^- + 4H^+ \rightarrow 2H_2O \qquad (2)$$

Water is produced by this oxygen reduction reaction at the cathode. This water must be transported away from the cathode catalyst layer into the gas flow channel where it is convected out of the cell (Figure 2) [4]. The gas diffusion layer is responsible for this important function.

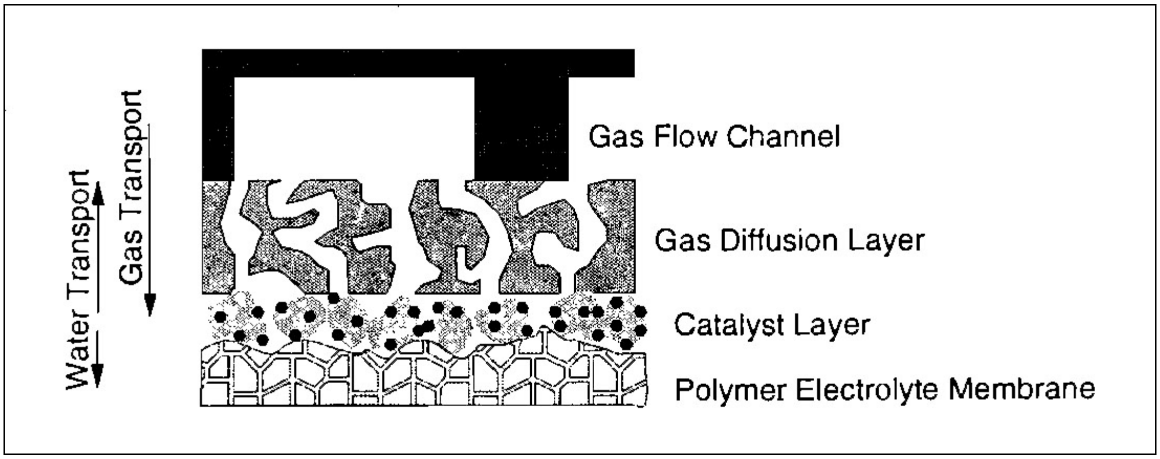

**Figure 2. Oxygen or air flows through the gas flow channel, and must diffuse through the gas diffusion layer to the catalyst layer where it reacts with protons coming through the polymer electrode membrane to make water. The water formed must go from the catalyst layer to the gas diffusion layer into the gas flow channel where it can be convected out of the fuel cell. Some water may also enter the polymer electrolyte membrane.**

There is water flow in the two inlet gas channels, the two GDLs, and the membrane [5]. However, the accumulation of water produced at the catalyst/membrane interface is very important to the performance of the cell. Lin and Nguyen report that two thirds of the total voltage loss in a PEM fuel cell can be attributed to the cathode's poor performance [6]. The oxygen reduction rate at the cathode is the limiting kinetic step and determines how much current can be generated. During the operation of the cell, the rate depends on the transport rate of oxygen from the cathode flow channel through the GDL to the catalyst layer [7]. The GDL plays the essential role of permitting oxygen gas to be transported from the cathode gas supply channel to the interface between the electrolyte membrane and the catalyst. The rate of this transport is greatly reduced when liquid water accumulates in the cathode [6]. Some simulation studies have suggested that that liquid water can block the gas pores needed for oxygen gas transport within the gas diffusion and catalyst layers as well as cover the catalyst active surface required for the cell reaction [5]. This can only happen if the GDL is made from a hydrophilic material, then water will readily enter the pores of the GDL. Water that has condensed in the GDL pores will hinder diffusion of oxygen to the cathode catalyst/membrane interface by blocking access to the oxygen gas. However, if the GDL is made from a hydrophobic material, water produced at the cathode will be inhibited from entering the pores of the GDL so oxygen diffusion to the catalyst surface is not impeded. The product water will build up at the interface because a hydrophobic GDL will not readily allow water to enter the pores of the GDL. In order for water produced at the cathode to be removed from the catalyst/electrode interface, a driving force is needed to push the water through the GDL.

In a PEM fuel cell with a hydrophobic GDL, the water produced by the oxygen reduction reaction is not permitted to enter the GDL and builds up at the interface between the cathode catalyst and the polymer membrane. The membrane absorbs this water and swells. The swelling can compress the GDL, and this pressure will eventually be sufficient to force the water through the hydrophobic GDL.

In addition to providing oxygen gas access to the catalyst layer and passage for removal of product water, the GDL must also provide electronic conductivity, heat conductivity, and mechanical strength [8]. The GDL should have mechanical strength to (1) provide mechanical support for the polymer electrolyte membrane in the case of reactant pressure difference between the anode and cathode gas channels, (2) maintain good contact with the catalyst layer, and (3) to not compress into the gas flow channels that would result in blocked flow and high channel pressure drops [8]. According to Mathias *et al.*, the most promising candidates for use as diffusion media in PEM fuel cells are carbon-fiber-based products, such as non-woven papers and woven cloths, due to their high porosity and good electrical conductivity [8]. In industry, carbon paper is most commonly used to make gas-diffusion electrodes for phosphoric acid fuel cells, and carbon cloth is used to prevent friction and wear in automotive transmissions and aircraft brakes [8].

Previous work by Benziger, *et al.* suggest that the GDL consists of pores with varying size that run between the catalyst layer and the gas flow channel [9]. The idealized picture they presented assumed that the pores are cylindrical and run transverse across the GDL. When water diffuses through a cylindrical pore, it wets the wall of the pore. Hydrophilic walls allow the water to be drawn into the pores and condense in the GDL before it can accumulate at the interface of the electrode and the polymer electrolyte. A hydrophilic GDL does not restrict the water flow, and flow will be observed at any pressure. However, if the pore walls are hydrophobic, water flow is restricted and water does not enter the pore until a sufficient pressure is applied to overcome the surface energy. The carbon fiber materials are slightly hydrophobic. In order to improve the gas and water transport within the gas diffusion later, it is commonly treated with a hydrophobic agent such as polytetrafluroethylene (PTFE or Teflon) to increase the hydrophobicity [6]. Coating the fibers with Teflon makes the pores highly hydrophobic and requires an even greater pressure to achieve water flow.

In order for the GDL to effectively transport reactant gas from the gas supply channel to the membrane/catalyst interface, the GDL must maintain free void volume for the diffusive flow of gas. Previous work by Benziger, *et al.* has concluded that when sufficient pressure is applied, the largest pores of the GDL are preferred to push the water through. This is because the larger pores require less work to overcome the unfavorable surface energy [9]. This implies that smaller pores are left free to transport reactant gas to the reaction site in the cell.

In the current research, various gas diffusion media were placed under hydrostatic pressure in order to directly observe and record water being pushed through the gas diffusion layer. The development of water droplets and their consequent detachment were observed. This is of great interest to understanding water management in the fuel cell. Current research conducted by Erin Kimball indicates that water droplets forming in the gas flow channel combine with other droplets as they are detached from the GDL to form slugs that greatly affect the performance of the fuel cell. The cell's performance depends on the orientation of the cathode. When the cell is oriented vertically and slugs are pulled out of the gas flow channel with gravity or an airflow great enough to clear the slugs is applied, the energy output is stable. However, if the cell is oriented horizontally or an airflow against gravity is applied, instabilities are observed. When these conditions are present, the gas flow channel becomes partially or fully flooded, blocking the transport of reactant gas through the GDL and to the reaction site. It is important to understand the physics of how water droplets form at and detach from the GDL and to measure the forces involved in this phenomenon. The critical detachment sizes of the water droplets are measured, and a theoretical pore size for the samples are calculated and reported. This paper also reports measurements of the minimum pressure required to push water through the various GDL media and water flow rates as a function of pressure.

## II. Experimental

The gas diffusion media observed in this experiment were provided by E-TEK (E-TEK Division of De Nora N.A., Inc. 39 Veronica Ave., Somerset, NJ 08873 USA). Carbon cloth with 20% Teflon wet-proofing and 0% Teflon wet-proofing and Carbon Toray paper with the same loadings were obtained.

A flow visualization cell was designed to house a sample of gas diffusion material and allow water to collect on one side of the gas diffusion media and build hydrostatic pressure. The schematic of the design for the flow visualization cell is shown in Figure 3 and Appendix III, and a photograph is shown in Figure 4. There is a chamber in which the gas diffusion material is held in place by a plate and O-rings. Silicone sealant was used around the edges of the material in order to prevent water from leaking around the material.

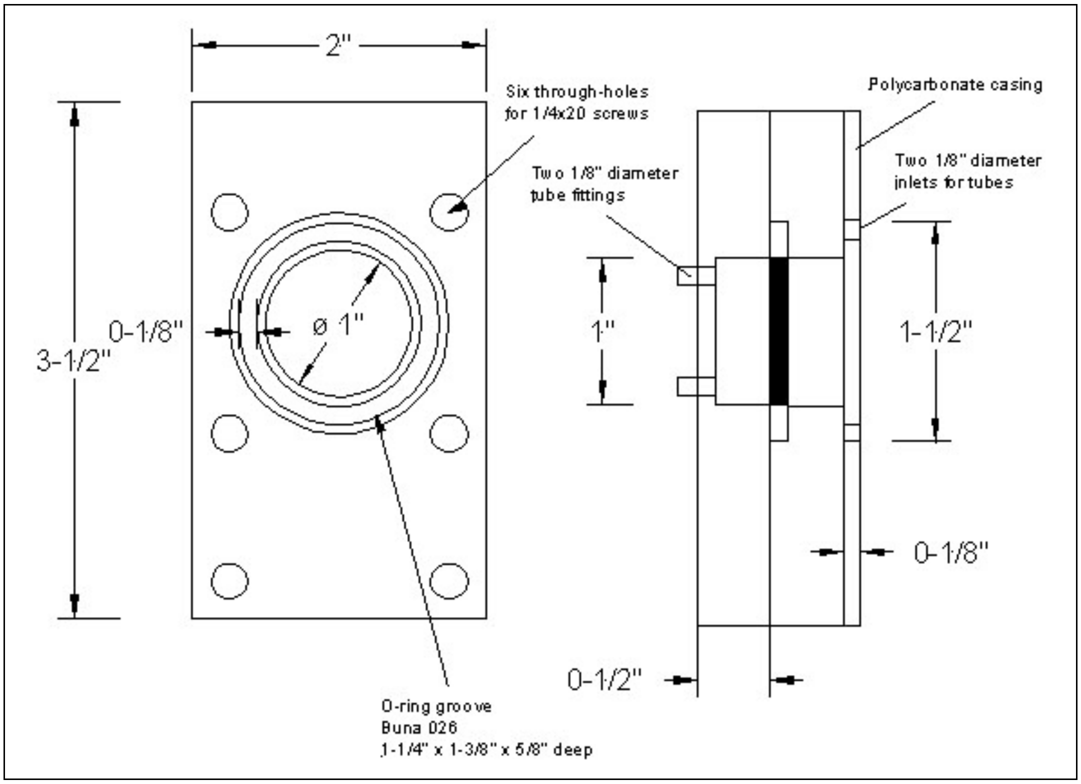

**Figure 3. Design of Flow Visualization cell.**

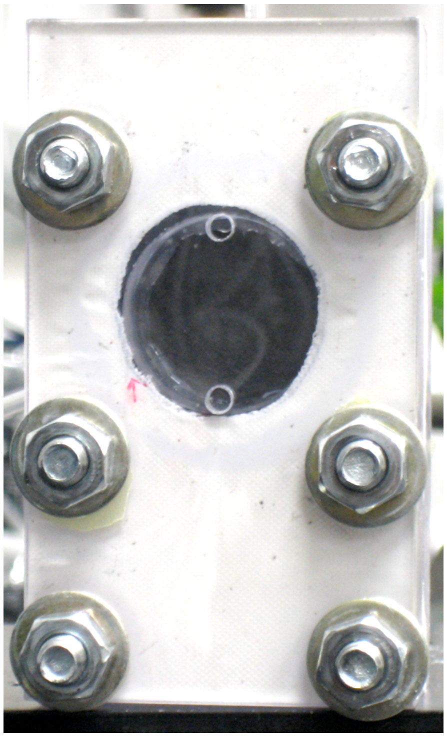

**Figure 4. Camera-side or "gas side" of the flow visualization cell. The gas diffusion media was video recorded through a polycarbonate cover.**

Water enters the unit on the non-camera side or "catalyst side" through a 1/8-inch Tygon tube. A clear Tygon tube was connected between the unit and a large reservoir of water that was placed on a platform jack. Pressure in the flow visualization cell was manipulated by adjusting the height of the jack. A long clear Tygon tube exposed to air was connected to the top of the unit. The height of the hydrostatic head was measured with a tape measure affixed to the wall, and pressure was calculated using Equation 3.

$$\begin{aligned} \Delta P &= \rho g h \\ h &= \text{height of water column} \end{aligned} \tag{3}$$

A schematic and photograph of the experimental set-up are shown below in Figure 5 and Figure 6. On the other side of the gas diffusion media was a 1-inch diameter view window covered with a thin piece of polycarbonate (Figure 3). Polycarbonate was chosen as the material for this flow visualization cell because of its transparency, so the gas diffusion media could be viewed and video-recorded. The video camera was positioned so water droplet formation on the gas diffusion media could be video-recorded once sufficient pressure was reached to overcome the surface energy of the pores (Figure 7).

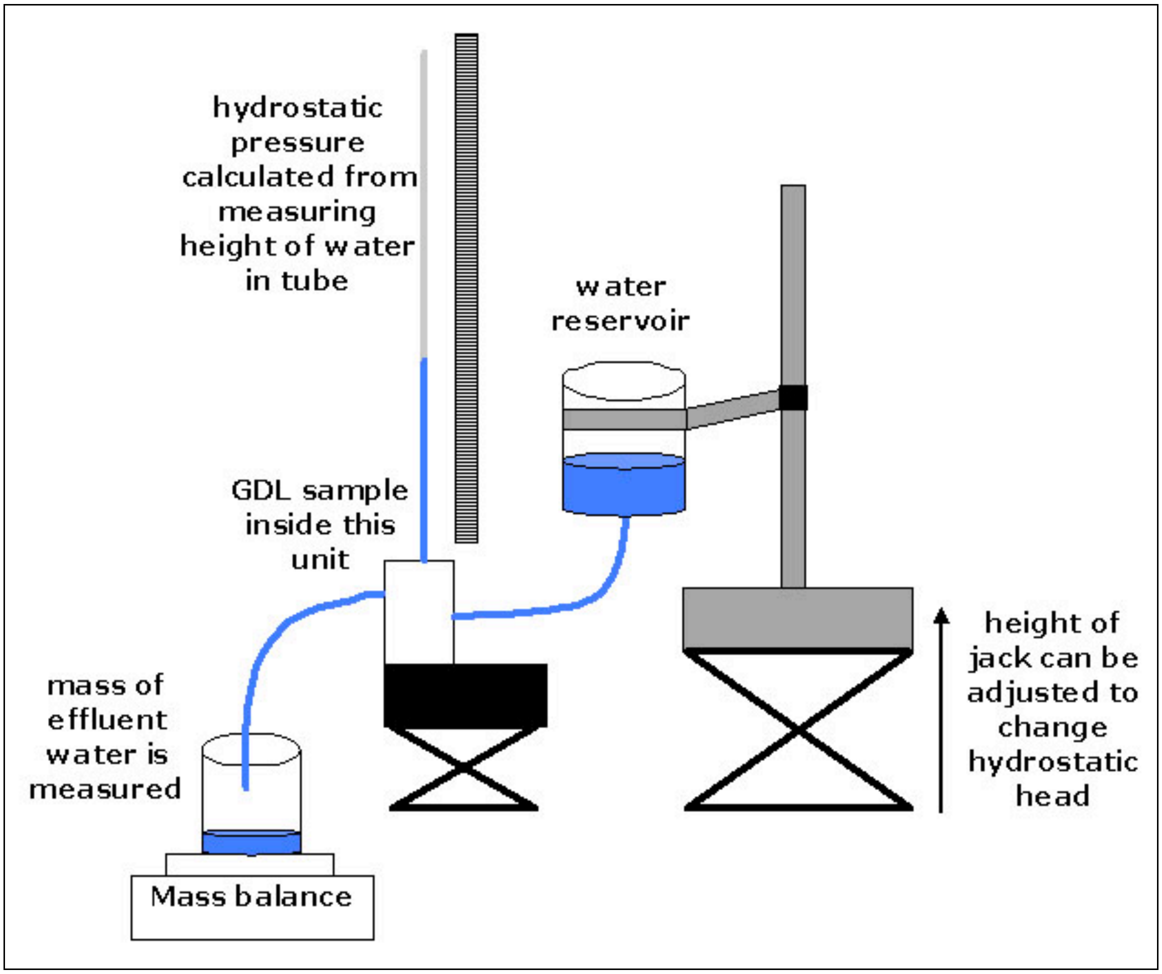

**Figure 5. The GDL sample is housed in a unit where water enters from a reservoir of water. The reservoir of water is connected to a ring stand on a moveable jack whose height can be adjusted in order to change the hydrostatic head. A Tygon tube is connected to the unit housing the GDL sample. The pressure is calculated from measuring the height of the water in the tube with a measuring tape affixed to the wall directly behind the set-up.**

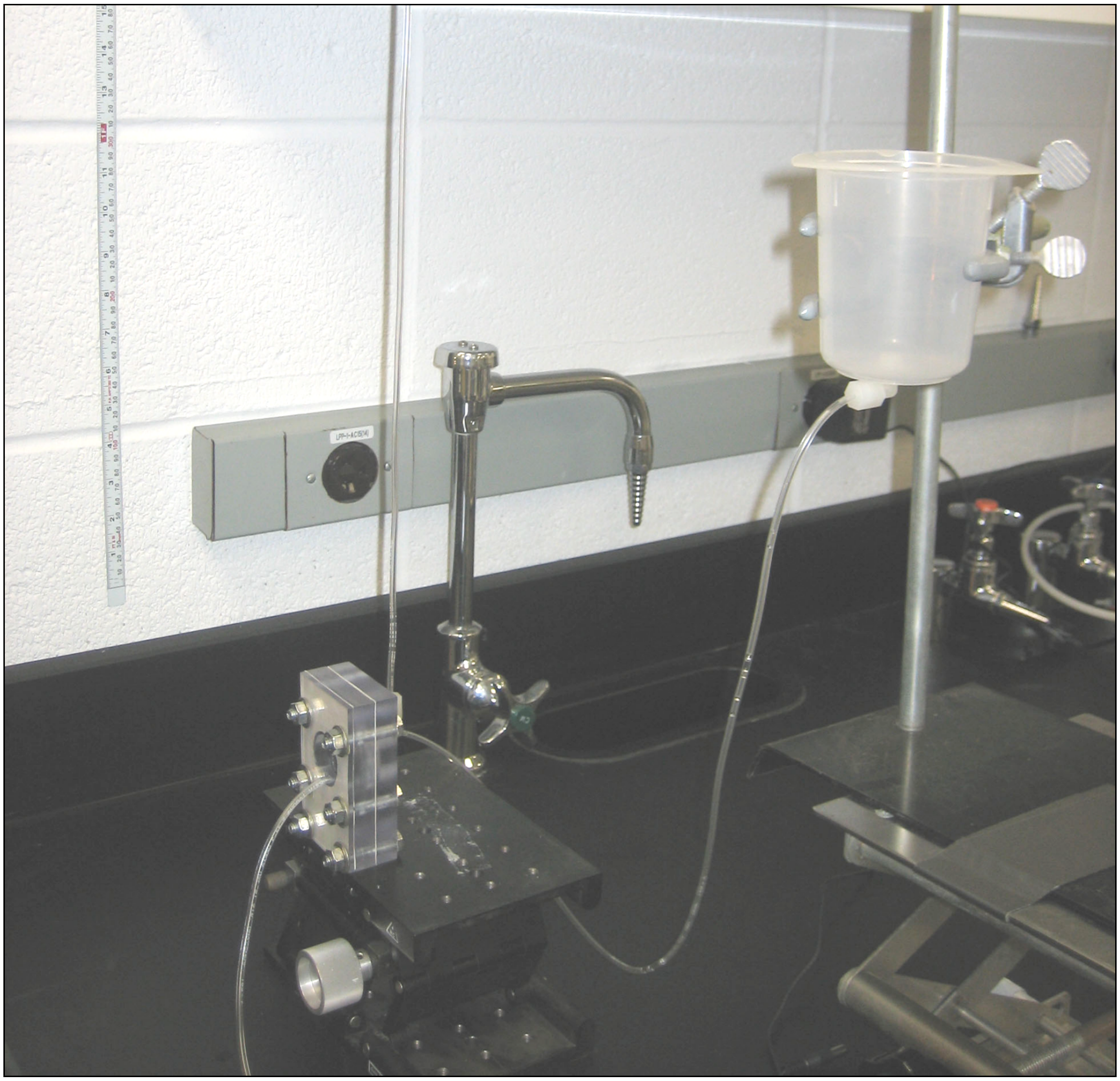

**Figure 6. Photograph of experimental set-up.**

**Figure 7. The camera was positioned to capture water droplet formation and detachment on the "gas side" of the membrane.**

This minimum pressure was recorded for each type of gas diffusion media. The formation of water droplets and flow of water through the GDL was recorded in short 10-30 second intervals at the critical pressure for water flow and various pressures above this critical pressure. A tube was attached to the top of the view window to flow oxygen at a small rate to provide enough force to push the effluent water from the viewing area and to a beaker. The effluent water collected in the beaker was weighed every 5 seconds so water permeation rates could be calculated. These measurements were taken at a variety of pressures over the course of 5-12 minutes. The experiment was repeated after allowing the water to drain from the unit. These "wet" measurements were taken without drying the gas diffusion media. The experiment was also carried out after the gas diffusion media was dried in place with nitrogen gas for 2.5 hours. Water flow through the carbon paper GDL was observed and video-recorded for 2-3 minutes at various pressures in order to establish an average frequency of water droplet formation and critical droplet detachment size as a function of pressure.

## III. Results

The minimum pressure required for water flow through the GDL was recorded for each type of gas diffusion media (Carbon paper with 0% and 20% Teflon wet-proofing and carbon cloth with 0% and 20% Teflon wet-proofing). After allowing the water to drain from the experimental cell, the experiment was repeated without drying the gas diffusion media. The experiment was repeated after the GDL material was dried in place with nitrogen. The results are summarized in Table 1.

The results from the repeated experiments performed without drying the GDL material confirm that there is a decrease in the necessary pressure head to cause water flow through the material compared to an initially dry sample. The results also confirm that there is a small decrease in the necessary pressure to cause flow between an unused sample that is initially dry and a previously used sample that is initially dry.

**Table 1: Minimum Pressure for Water Flow through Gas Diffusion Media**

| **GDL Media Sample** | **Minimum pressure for flow in a *virgin* GDL (Pa)** | **Minimum pressure for flow in a *wet* GDL (Pa)** | **Minimum pressure for flow in a *previously used dried* GDL (Pa)** |
|---|---|---|---|
| Carbon paper + 20% Teflon | 8400 | 3800 | 6000 |
| Carbon cloth + 20% Teflon | 1700 | 1500 | 1200 |
| Carbon paper | 4000 | 1500 | -- |
| Carbon cloth | 1700 | 1100 | 1400 |

The mass of the effluent water from the flow visualization cell was measured every 5 seconds for 8-12 minutes, and from this data, the average mass flow rate was calculated. After observing water flow at the critical pressure, the pressure was increased and mass flow measurements were taken. The results indicate that mass flow rates increase as pressure is increased. A summary of the results can be found in Table 2.

**Table 2: Flow rate of water through GDL at various pressures**

| Run | Material | Wet proofing | Pressure (Pa) | Flow rate (g/min) |
|---|---|---|---|---|
| Dry | Carbon cloth | 20% | 1650 | 1.2 |
| Dry | Carbon cloth | 20% | 1850 | 1.5 |
| Wet | Carbon cloth | 20% | 1950 | 3.4 |
| Dried in $N_2$ | Carbon cloth | 20% | 1950 | 1.8 |
| Dry | Carbon paper | 20% | 9600 | 0.62 |
| Dried in $N_2$ | Carbon paper | 20% | 7700 | 0.50 |
| Dry | Carbon paper | 20% | 8450 | 0.27 |
| Wet | Carbon paper | 20% | 3800 | 0.20 |
| Dried in $N_2$ | Carbon paper | 20% | 6000 | 0.22 |

Each experiment was recorded for 15-30 second intervals to directly observe where water droplets formed, i.e. whether there was a preference for certain pores, and when droplets would detach from the GDL material. The video recordings indicate that for each sample, there are a small number of pores that allow water permeation. At the minimum pressure where water flow was first observed, water droplets usually only formed at one pore. Images of water flow through selected pores can be found in Figure 8 and also in Appendix I and Appendix II. Short video clips between 15 and 30 seconds long indicate that water flow occurs at the same pores for each sample, and longer recordings of 2-3 minutes indicate the same. It was often the case that for each sample, even after draining the unit or drying the GDL material in nitrogen, water flow occurred through the same pores.

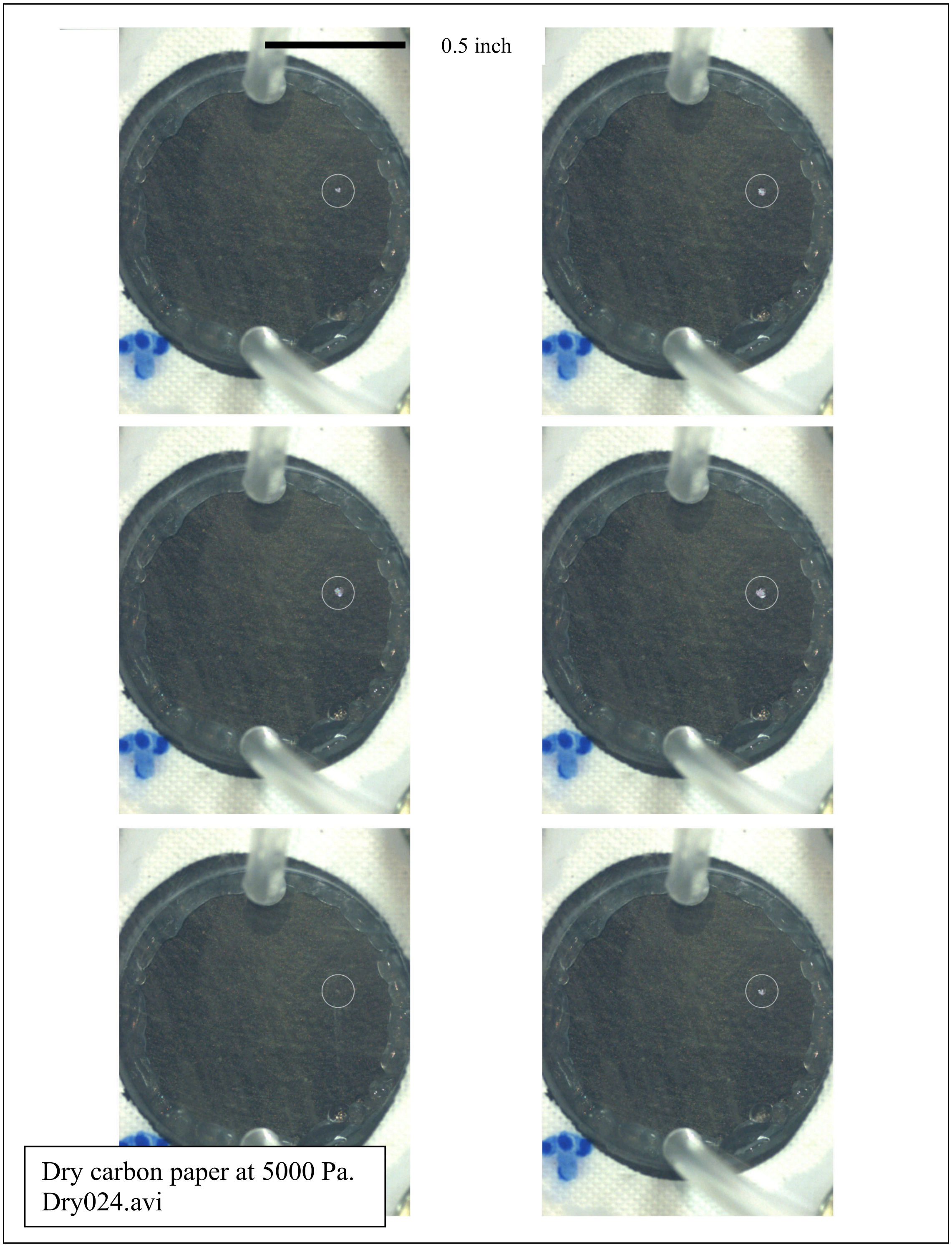

**Figure 8. At the minimum pressure for water flow, water only flows through selected pores. In this case, only one pore is chosen for water flow. Water will flow where there is the smallest amount of surface energy to overcome. The water droplet evolves from the same pore as demonstrated in this figure.**

When pressure was kept constant, the water droplets formed with regular frequency. As indicated earlier, as the hydrostatic pressure on the GDL sample was increased, the mass flow increased. In some instances, as the pressure was increased, this meant that the frequency of the water droplet formation through the preferred pore(s) increased. In most instances when pressure was increased, new pores would allow water to flow through the media (Figure 9). Multiple drop formation limited our ability to determine the frequency of droplet formation and detachment. When water flowed through several pores located close together, like the situation in Figure 8b, droplets would coalesce with droplets forming close by.

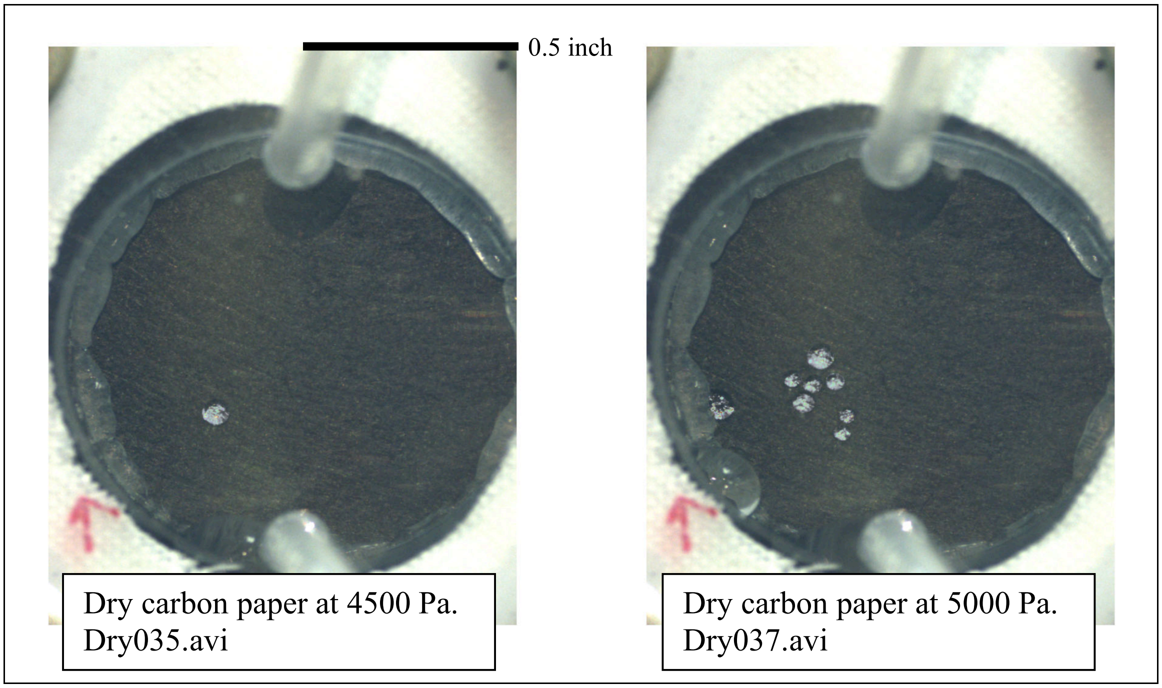

Dry carbon paper at 4500 Pa.
Dry035.avi

Dry carbon paper at 5000 Pa.
Dry037.avi

**Figure 9. Many times, when the hydrostatic pressure head was increased, water flow would happen at new pores. These droplets would coalesce. The image on the left was taken under P = 4500 Pa. The image on the right was taken under P = 5000 Pa.**

The water droplets detached from the surface of the GDL material with regular frequency. Water flowing through the pores of the GDL material would build up at the surface of the GDL. The droplets had to reach a critical size in order to detach from the GDL material. Once detached, the water droplets fell straight down to the effluent tube where they were collected in a beaker.

## IV. Discussion

The experimental results reveal that water flow happens at certain pores. These pores are the largest in the GDL sample. The largest pores have the smallest surface energy and require the least amount of pressure in order to push the water through. Once water enters the pore, the resistance against penetration is no longer present, and water flow will continue even after the hydrostatic pressure is slightly reduced. If the hydrostatic pressure is increased, water flow is observed at more pores as the hydrostatic pressure is large enough to overcome higher surface tensions at smaller pores. Once the water is pushed through the pore, a water droplet forms at the surface of the GDL. As water continues to flow, the water droplet increases in size until it reaches a critical size and detaches from the surface of the GDL. Water droplets forming at these pores have a consistent radius required for detachment. The critical radius for carbon paper and carbon cloth at the onset of water flow is reported in Table 3.

We have chosen to model the water droplet forming at the surface of the GDL material as a spherical mass of water attached to the surface of the GDL that builds mass as water flows through the pore. The surface energy of the water keeps the droplet attached to the surface of the GDL material. Detachment occurs only when the droplet has reached a critical size, when the force due to gravity on the mass has overcome the surface energy keeping the droplet attached to the surface of the GDL. A schematic of this model can be found in Figure 10.

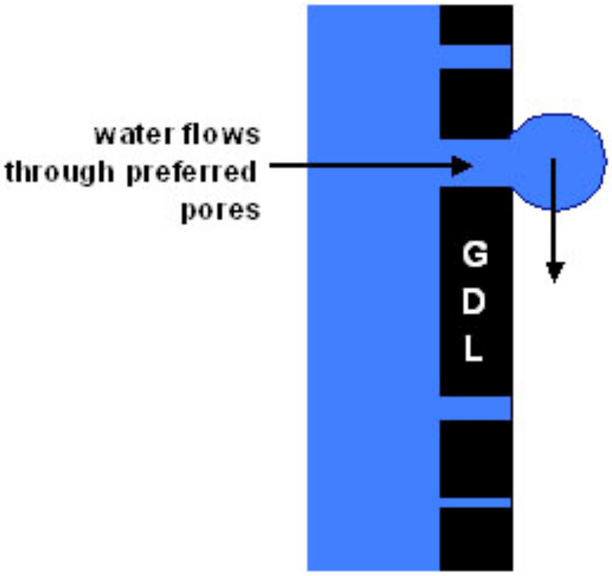

**Figure 10. Model of water droplet detachment. The water droplet will detach from the surface of the GDL material once it reaches a critical size. At this critical size, the force of gravity on the mass of the droplet overcomes the surface energy holding the droplet attached to the GDL surface.**

The condition for detachment is written in Equation 4.

$$(V_{drop})\rho g = 2\pi(r_{pore})(\gamma_{water/air}) \tag{4}$$

Droplet formation and detachment for carbon paper and carbon cloth were video recorded. The video was converted to a sequence of images so that the radii of the droplet could be measured as a function of time. It was of particular interest to calculate the critical droplet size for detachment at the onset of water flow. The radius of the droplet immediately before it detached from its pore location was recorded, and the volume was calculated assuming the droplet was spherical. These measurements were used to calculate the pore radii for these samples using the model described above. In calculating the radius of the pore, we assume that the surface energy between the air and the water droplet is 70 dynes/cm, and the droplet is spherical. The radius of the pore is calculated by using Equation 5. $V_{drop}$ is the volume of the droplet immediately before the droplet detaches.

$$r_{pore} = \frac{(V_{drop})\rho g}{2\pi(\gamma_{water/air})} \tag{5}$$

Using Equation 5, the calculated pore size for the carbon paper is 125 ± 6 μm, which is consistent with what was found in the previous work completed by Benziger, *et al.* [9]. The calculations from previous work were based on the minimum pressure head required for water flow through each sample using the Young and Laplace Equation (Equation 6).

$$\Delta P = \frac{2\gamma_{water}\cos\theta}{r_{pore}} \tag{6}$$

In this study, the pore size of the carbon cloth calculated from direct measurement of the water droplet radii is 185 ± 6 μm. Previous reports say the radii of the pores preferred for water flow through a sample of carbon paper is 140 μm [9], which is the same order of magnitude as the pore radii calculated here. The critical radii of the droplets for detachment are presented in Table 3. This measurement was taken from video recordings of both carbon paper and carbon cloth at the minimum pressure for water flow. The calculated pore radii and the pore radii previously reported are presented in Table 3. As reported in Table 1, the water permeation rate is higher for the carbon cloth than the Toray paper because the pore sizes for the carbon cloth are higher. Larger pores allow more water to flow out over time.

**Table 3: Measurements for droplet radii at the onset of water flow. The calculation of the pore radius is compared to calculations previously reported.**

| GDL Material | Droplet critical radius (μm) | Pore radius based on droplet radius (μm) | Previously reported Pore radius (μm) |
|---|---:|---:|---:|
| Carbon cloth | 1250 | 185 | 140 |
| Carbon paper | 600 | 20 | 21 |

Once the water droplets reached a critical size and detached from their original location, the water fell straight down to the effluent tube. The hydrophobicity of the GDL material prevented the water from attaching to other parts of the GDL surface. If water flow was happening through several pores, a falling water droplet from one location would coalesce with another water droplet forming at another location. This would most times immediately result in the combined water droplet detaching from the GDL because the mass of the combined water droplet was very large.

By measuring the radii of the droplets and calculating the radii of the pores where the droplets form, we have a direct way to calculate the volumetric flow rate through the pore. First, it is assumed that water flow through the pore can be modeled as laminar. Second, it is assumed that the pore can be modeled as a cylindrical channel with length being the thickness of the GDL material. Under these assumptions, the volumetric flow rate is given by Equation 7.

$$Q = \frac{\pi \, \mathrm{r}_{\mathrm{pore}}{}^{4}}{8\mu \mathrm{L}} \Delta \mathrm{P} \qquad (7)$$

We assume the surface energy of water is 70 dynes/cm and the water's viscosity is 0.01 g/cm-s. Furthermore, it is assumed that the pressure required for flow must overcome the surface energy that prevents water flow through the pore. The pressure is give by the Young and Laplace Equation (Equation 6 reprinted below). Therefore the flow rate through a pore in the GDL material is given by Equation 7.

$$\Delta \mathrm{P} = \frac{2\gamma_{\mathrm{water}} \cos\theta}{\mathrm{r}_{\mathrm{pore}}} \qquad (6)$$

$$Q = \frac{2\pi\gamma}{8\mu \mathrm{L}} r_{pore}{}^{3} \qquad (7)$$

The volumetric flow rates calculated from the pore sizes reported in Table 3 are presented in Table 4. These flow rates represent the theoretical volumetric flow rate through one pore. These values differ from the ones reported in Table 1 because the pressure was sufficiently high to cause water flow through more than one pore.

**Table 4: Volumetric flow rate through one pore.**

| GDL Material | Pore radius (cm) | Thickness (cm) | Volumetric flow rate ($cm^3$/min) |
|---|---|---|---|
| Carbon cloth + 20% Teflon | 0.0185 | 0.036 | 0.60 |
| Carbon paper + 20% Teflon | 0.00200 | 0.038 | 0.00072 |

## V. Conclusion

Liquid water transport occurs at the largest pores because they require the least amount of pressure to push the water through. From the video recordings, one can see that water droplets form at the same pores over time, and even after drying the GDL sample. Our model of droplet detachment helps explain the conditions for detachment and provides a way to calculate the radius of the pore through which water penetrates. It assumes that the force of gravity overcomes the surface energy that keeps the droplet attached to the surface of the GDL material. It also assumes that the droplets are spherical. The calculations agree well with previously reported calculations for the size of the preferred pores for carbon paper and carbon cloth.

Our model for water flow through the pores did not agree well with the data collected. The model assumed that flow through the pore was laminar and that the pores were cylindrical channels with length equal to the thickness of the GDL sample. These assumptions are not good approximations, and the calculated flow rates did not scale as the pore radius cubed.

## VI. Bibliography of Works Cited

[1] He, Yi, Nguyen, AIChE Two-phase Flow Model of the Cathode of PEM Fuel Cells Using Interdigitated Flow Fields 46 (2000).

[2] Larminie, Dicks, Chapter 2: Efficiency and Open Circuit Voltage, in: Fuel Cell Systems Explained, John Wiley & Sons, 2003, pp. 1-24.

[3] Chia, Benziger, Kevrekedis, AIChE Water Balance and Multiplicity in a Polymer Electrolyte Membrane Fuel Cell 50 (2004) 2320-2324.

[4] Benizger, Schematic of cathode side of the membrane-electrode assembly, in: Water flow in the gas diffusion layer of PEM fuel cells, Journal of Membrane Science, 2005.

[5] Springer, Zowodzinski, Gottesfeld, Journal of the Electrochemical Society Polymer Electrolyte Fuel Cell Model 138 (1991) 2334-2342.

[6] Lin, Nguyen, Journal of the Electrochemical Society Effect of Thickness and Hydrophobic Polymer Content of the Gas Diffusion Layer on Electrode Flooding Level in a PEMFC 152 (2005) A1942-A1948.

[7] He, Lin, Nguyen, AIChE Diagnostic Tool to Detect Electrode Flooding in Proton-Exchange-Membrane Fuel Cells 49 (2003) 3221-3228.

[8] Mathias, Roth, Fleming, Lehnert, Diffusion media materials and characterisation, in: Handbook of Fuel Cells Fundamentals, Technology and Applications, vol 3, Wiley & Sons, Chichester, 2003, pp. 517-537.

[9] J. Benziger, Journal of Membrane Science Water flow in the gas diffusion layer of PEM fuel cells 261 (2005) 98-106.

## **Appendix I** P = 8000 Pa; Dry virgin sample of Toray paper dry007.avi

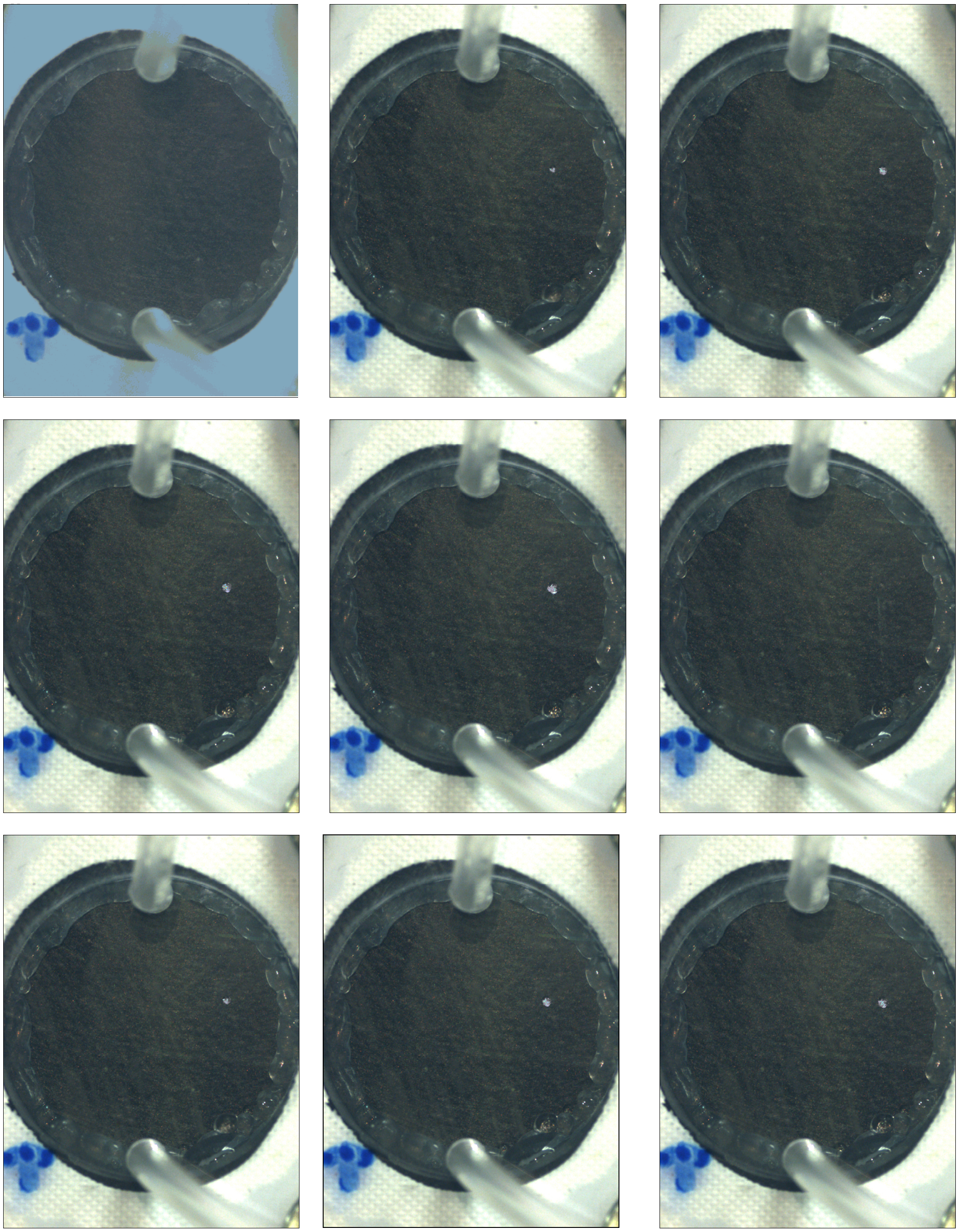

## **Appendix I** P = 8000 Pa; Dry virgin sample of Toray paper dry007.avi

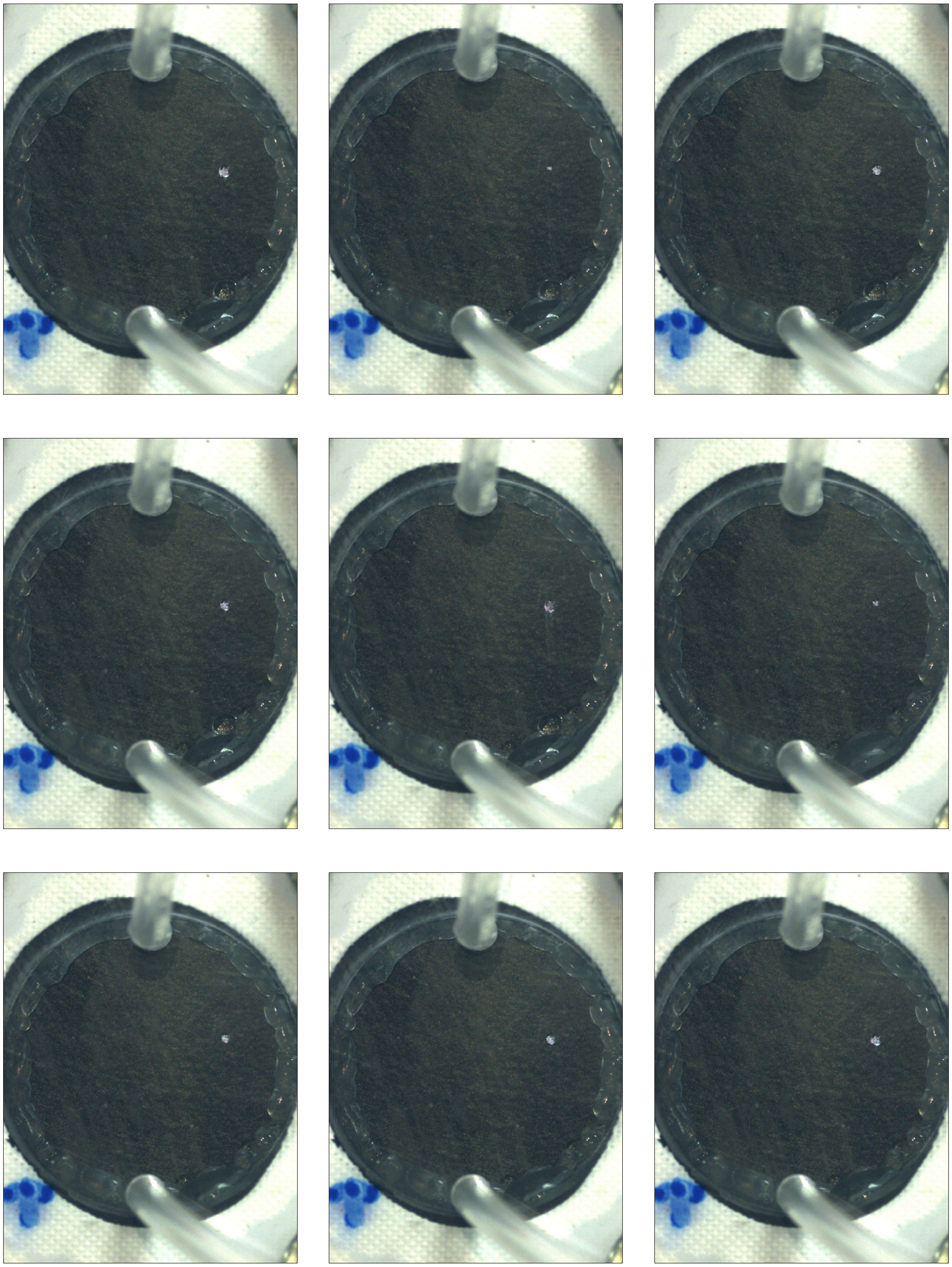

**Appendix I** P = 8000 Pa; Dry virgin sample of Toray paper dry007.avi

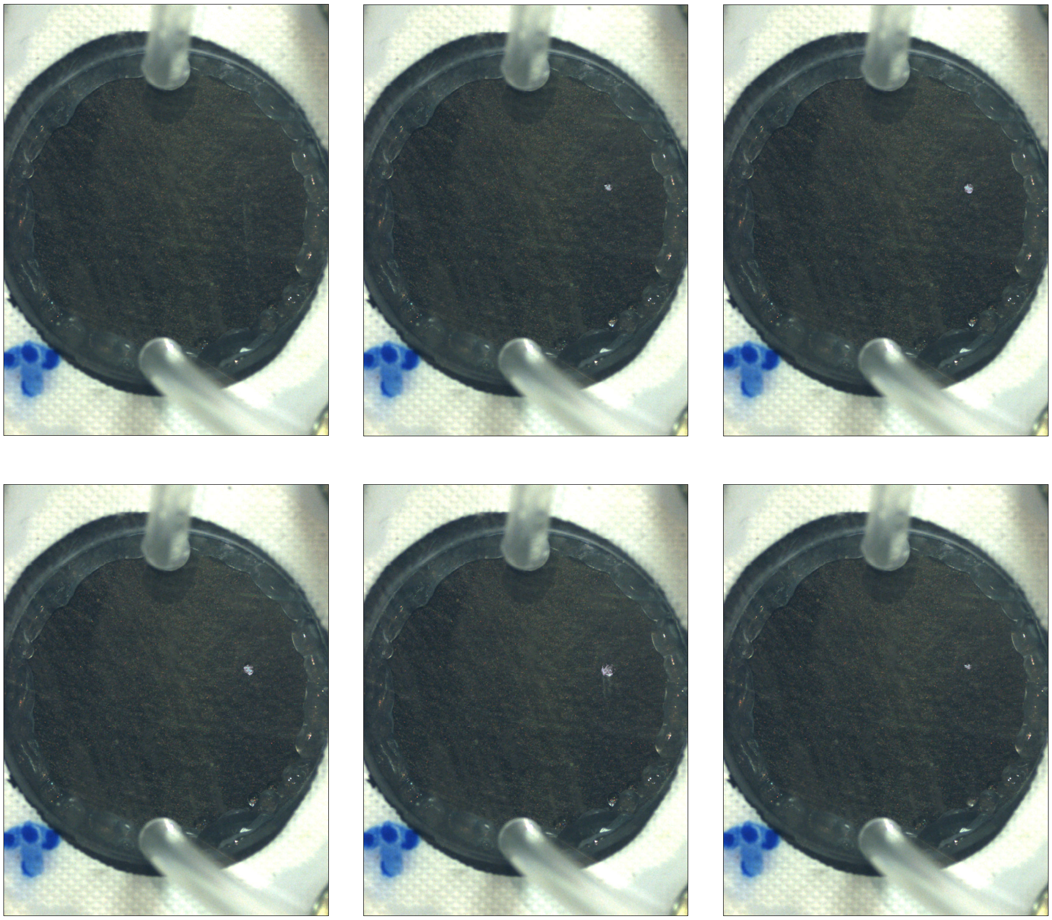

**Appendix II** P = 1700 Pa; Dry virgin sample of carbon cloth dry024.avi

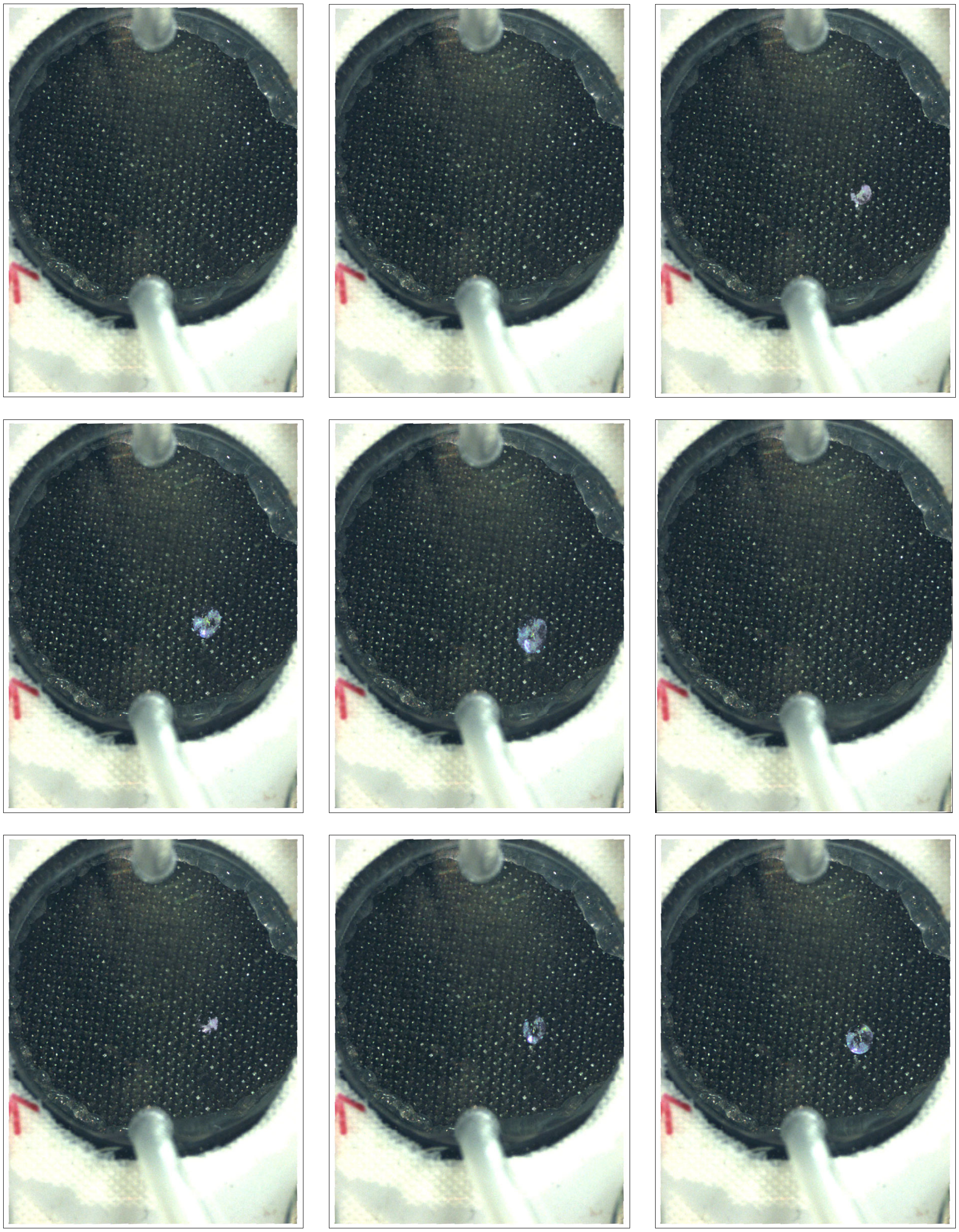

## **Appendix II** P = 1700 Pa; Dry virgin sample of carbon cloth dry024.avi